Weighted L1 and L2 Norms for Image Reconstruction: First Clinical Results of Electrical Impedance Tomography Lung Data

Peyman Rahmati[1], Andy Adler[1]

[1]Dept. of Systems and Computer Eng. Carleton University, Ottawa, ON., Canada.
E-mail: {prahmati, adler}@sce.carleton.ca

March 6, 2013

Abstract: Image reconstruction is an inverse problem which can be formulated using quadratic objective functionals (Least Square fittings or L2 norms) and absolute values summations (L1 norms). The L1 and L2 norms can be independently applied over the data mismatch and the regularization terms (image term) of an inverse problem. In this manuscript, we investigate weighted L1 and L2 norms in constituting a general inverse problem and reconstruct image using Primal-Dual Interior Point Method (PDIPM). We propose a generalized inverse problem to independently mix the smooth properties of the L2 norm based objective functionals with the blocky effect of the L1 norm based objective functionals on a element by element basis through a weighting strategy. In our implementation, we use Electrical Impedance Tomography (EIT) as an instance of ill-posed, non-linear inverse problem. We investigate the effectiveness of different combinations of weighted L2 and L1 norms in dealing with measurement uncertainties, such as measurement noise and data outliers, using both EIT simulated data, and EIT human lung data. The simulated data is produced for a 2D circular phantom and EIT conductivity images are reconstructed. The first clinical results of applying weighted L1 and L2 norms to reconstruct image of EIT lung data using a 2D thorax-shape mesh are reported.

1 Introduction

Inverse problem is to infer unknown or hard to determined parameters of a system from experimental observations or data points. The unknown system parameters define the properties of the system and are not directly measurable. The experimental observations are easily measurable and their values depend on the value of the unknown parameters through a linear or non-linear relationship, depending on the physical laws governing the system. Forward model is the linear or non-linear relationship that link the system parameters to the measured data or observations. Three source of information are needed to solve an inverse problem: 1) the forward model, 2) the observed data (d), defined on the data space D, 3) the priori information about the unknown system parameters (m), defined on the model space M. The latter is the most important source of information which is usually hard to determine. An accurate selection of prior information about the unknown system parameters highly stabilizes the inversion solution. In this manuscript, we aim to discuss a broader perspective of the possible deterministic inverse problems through proposing a generalized inverse problem solved by the PDIPM framework. We propose a generalized inverse problem which mixes the L1 norms and the L2 norms on both the data and the regularization terms of an inverse problem. To reach to the maximum generality, the norms are weighted to enclose the maximum number of possible categories of inverse problems. In the following, we discuss our proposed generalized inverse problem with weighted L1 and L2 norms.

2 Generalized inverse problem with weighted L1 and L2 norms

In this section, We formulate a general solution for a general inverse problem using PDIPM framework. A general primal minimization problem can be written as set of error functions as follows

$$(P) = \text{argmin}\{\zeta \sum_{i=1}^{D_1} |f_{d_i}(m)| + \eta \sum_{j=1}^{D_2} |f_{p_j}(m)| +$$

$$(1\text{-}\zeta) \|g_d(m)\|^2 + (1-\eta) \|g_p(m)\|^2\}; \quad (1)$$

where ζ and η are weighting variables in the range $[0,\ 1]$. $f_d(m)$ is a L1 norm based data mismatch term, $f_p(m)$ is a L1 norm based regularization term, $g_d(m)$ is a L2 norm based data mismatch term, and $g_p(m)$ is a L2 norm based regularization term. A primal minimization problem can be formed through any combination of the error terms defined in (1). In the following, the general solution for the general primal problem in (1) is derived using PDIPM framework.

The dual problem can be written as

$$(D) = \underset{m}{\text{argmin}}\{max_{x_d}[\zeta x_d^T f_d(m)] + max_{x_p}[\eta x_p^T f_p(m)] +$$

(1-ζ)$\|g_d(m)\|^2 + (1-\eta)\|g_p(m)\|^2\}; |x_d| \leq 1, |x_p| \leq 1$(2)

the following objective functions can be considered: $f_d(m) = W\ (h(m) - d), f_p(m) = L\ (m - m_0), g_d(m) = W\ (h(m) - d), g_p(m) = \alpha\ L(m - m_0)$. α is the regularization parameter, W is a weighting diagonal matrix, $h(m)$ is the forward measurement, d is the measured data, L is the regularization matrix, m is the model parameter distribution or the primal variables, m_0 is a reference model parameter distribution. The smoothed PDIPM framework can be formulated as

$$C_d(m) = f_{d_i}(m) - x_{d_i}\sqrt{f_{d_i}(m)^2 + \beta} = 0,\ \forall i \quad (3)$$

$$C_p(m) = f_{p_j}(m) - x_{p_j}\sqrt{f_{p_j}(m)^2 + \beta} = 0,\ \forall j \quad (4)$$

$$|x_{d_i}| \leq 1, |x_{p_j}| \leq 1 \quad (5)$$

$$F_c(m) = \zeta\frac{\partial}{\partial m}(f_d(m))x_d + \eta\frac{\partial}{\partial m}(f_p(m))x_p +$$

(1-ζ)$\frac{\partial}{\partial m}(\|g_d(m)\|^2) + (1-\eta)\frac{\partial}{\partial m}(\|g_p(m)\|^2) = 0$(6)

the derived general PD framework above is solved iteratively using an iterative method, such as Newton method, and β decreases from points away from the region defined by the boundary $\|x_{d_i}\| \leq 1$ and $\|x_{p_j}\| \leq 1$ at every iteration, which is the notion of interior point methods. The Newton system to be iteratively solved to calculate the updates for the primal variables (m) and the dual variables (x_d and x_p) can be written as

$$\begin{bmatrix} \frac{\partial}{\delta m}F_c(m) & \frac{\partial}{\delta x_d}F_c(m) & \frac{\partial}{\delta x_p}F_c(m) \\ \frac{\partial}{\delta m}C_d(m) & \frac{\partial}{\delta x_d}C_d(m) & \frac{\partial}{\delta x_p}C_d(m) \\ \frac{\partial}{\delta m}C_p(m) & \frac{\partial}{\delta x_d}C_p(m) & \frac{\partial}{\delta x_p}C_p(m) \end{bmatrix} \begin{bmatrix} \delta m \\ \delta x_d \\ \delta x_p \end{bmatrix} =$$

$$- \begin{bmatrix} F_c(m) \\ f_d(m) - (\sqrt{f_d(m)^2 + \beta})x_d \\ f_p(m) - (\sqrt{f_p(m)^2 + \beta})x_p \end{bmatrix} \quad (7)$$

we define $f_d = f_p = f = h(m) - d$, $F = diag(f)$, $X = diag(x)$, $\kappa = \sqrt{f^2 + \beta}$, $E = diag(\kappa).g_d = g_p = g = L(m - m_0)$, $G = diag(g)$, $Y = diag(y)$, $s = \sqrt{(L(m - m_0))^2 + \beta}$, $S = diag(s)$. Replacing the defined objective functions into (7), we obtain

$$\begin{bmatrix} 2(1-\zeta)J^TW^TWJ + 2(1-\eta)\alpha L^TL & \zeta J^TW & \eta\alpha L \\ (I - XE^{-}1F)J & -E & 0 \\ (I - YS^{-}1G)L & 0 & -S \end{bmatrix}$$

$$\times \begin{bmatrix} \delta m \\ \delta x_d \\ \delta x_p \end{bmatrix} = - \begin{bmatrix} F_c(m) \\ f - Ex_d \\ g - Sx_p \end{bmatrix} \quad (8)$$

where matrix J is the sensitivity matrix. The primal variables (m) are updated in every iteration through a line search procedure which is written as $m^{(k+1)} = m^{(k)} + \lambda_m \delta m^{(k)}$, where k is the iteration number, δm is the update value with a descend direction to the optimal point, and λ is the step length [2]. In a similar manner, the dual variables (x_d and x_p) are also updated in every iteration. However, the direction of updates in the dual variables can be changed for different value of β at every iteration and may not be always ascending. Therefore, a line search procedure is not an appropriate method to update the dual variables. *scaling rule* is proposed to update the dual variables as follows [1]: $x^{(k+1)} = x^{(k)} + \min(1, \varphi^*)\,\delta x^{(k)}$, where φ^* is a scalar value such that $\varphi^* = \sup\left\{\varphi : \left|x_i^{(k)} + \varphi\,\delta x_i^{(k)}\right| \leq 1, \quad i = 1, \ldots, n\right\}$.

3 Experimental data

Electrical Impedance Tomography (EIT) is applied to reconstruct a conductivity distribution image of a 2D medium using the injection of electrical current into the medium and the collection of the resulting difference voltages across the electrodes attached to the boundary of the medium. We simulated EIT difference imaging with 16 electrodes with adjacent current stimulation pattern on one electrode plane discretized using a 2D circular finite element model (FEM) for the simulated data. A 2D human thorax-shape mesh was applied for the clinical data.

3.1 Simulated data

Figure 1 (a) shows the used 2D phantom to generate simulated data with 1024 mesh elements. The phantom contains two sharp inclusions with the two different conductivity values (0.9 S/m for the upper object and 1.1 S/m for the lower). The background conductivity value is 1 S/m. The inverse problem used the mesh density of 576 elements, which was different than the mesh density of the forward problem (1024 elements). The performance of the proposed generalized PDIPM for different weighting parameters was assessed based on two measurement conditions: 1) To account for the systematic errors and measurement noise of EIT data acquisition system, a zero mean Gaussian noise was added to EIT simulated data to produce a signal to noise ratio (SNR) of 60 dB, 2) To simulate the electrode error, caused due to electrode movement and electrode malfunction, a measurement failure rate of 0.5% was introduced, which means one measurement out of 208 measurements needed for one EIT frame was missed.

3.2 Clinical data

Clinical data were obtained in the study described by [4, 3]. The data includes human breathing data from eight patients with healthy lungs (age: 41 $\pm$ 12 years, height: 177 $\pm$ 8 cm, weight: 76 $\pm$ 8 kg, mean $\pm$ std.) and eighteen patients (age: 58 $\pm$ 14 years, height 177 $\pm$ 9 cm, weight: 80 $\pm$ 11 kg) with acute lung injury (ALI). All patients were intubated and mechanically ventilated. The experimental procedure consisted of a low flow inflation pressure-volume maneuver applied by the respirator (Evita XL, Draeger, Luebeck, Germany), starting at an expiratory pressure of 0 cmH2O and ending when either a) the gas volume reached 2L, or b) the measured airway pressure reached 35 cmH2O. Airway gas flow, pressure and volume were recorded at a sampling rate of 126 Hz. EIT data were acquired on sixteen self-adhesive electrodes (Blue

Sensor L-00-S, Ambu, Ballerup, Denmark), placed at the 5th intercostal space in one transverse plane around the thorax, while a reference electrode was placed on the abdomen. EIT data were acquired at 25 frames per second, with an adjacent stimulation and measurement protocol, using current stimulation at 50 kHz and 5 mA.

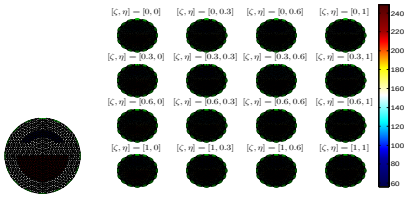

(a) (b)

Figure 1: EIT Image reconstruction using the proposed generalized PDIPM with weighted L1 and L2 norms over EIT simulated data perturbed by zero mean Gaussian noise (-60 dB). (a) 2D phantom. (b) The reconstructed images with different weighting parameters ($[\zeta, \eta]$).

4 Experimental Results

We show the EIT reconstructed images of the proposed generalized PDIPM framework with different selection of weighting parameters over both simulated and experimental data. The inverse solution is calculated using the proposed generalized PDIPM with $\beta = 1 \times 10^{-12}$. The stopping term to terminate the iterations depends on the value of the primal dual gap computed in every iteration of the PDIPM. According to our experiments, 10 iterations for the PDIPM were sufficient to reach to convergence. In our implementation, sixteen different selection for weighting parameters (ζ and η) are considered (figure 1(b)-4). The weighting matrix for ζ and η are selected as $[0, 0.3, 0.6, 1]$,including small, medium, and large weighting values. For every selection of weighting combination, the hyperparameter α was tuned up using L-Curve method [5]. Figure 1(b) shows the results over EIT simulated data when perturbed by a zero mean Gaussian noise (-60 dB). In figure 1(b), the upper panel on the left corner shows the result of solving the traditional L2L2 problem where $[\zeta, \eta] = [0, 0]$. The lower panel on the left corner is the solution of the L1L2 problem where $[\zeta, \eta] = [1, 0]$. The upper panel on the right corner represents the solution of the L2L1 problem; and the lower panel on the right corner shows the conductivity distribution image for the L1L1 problem. As it can be seen in figure 1(b), the reconstruction quality drops in the presence of added noise (-60 dB). Adding a Gaussian noise to EIT data, the reconstructed images with $\eta = 0$ (column 1 in figure 1(b)) become blurry and their image quality is dropped. The reconstructed images with larger weighting parameters (columns 2-4 in figure 1(b)) offer slightly higher robustness against the added noise and still provide sharp edges, as weights of the L1 norms and their contributions in the solution becomes higher from one column to another. A more challenging measurement condition was tested by adding noise (-60 dB) and data outliers, where one measurement out of 208 was missed, to the EIT simulated data.

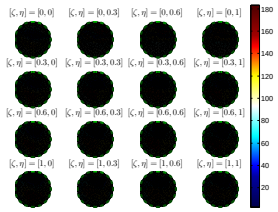

Figure 2: EIT Image reconstruction using the proposed generalized PDIPM with weighted L1 and L2 norms over EIT simulated data perturbed by zero mean Gaussian noise (-60 dB) and strong data outliers.

Figure 2 shows the reconstructed images for noise and data outliers test scenario. The weighting selection of either $\zeta = 0$ (row 1 in figure 2) or $\eta = 0$ (column 1 in figure 2) does not tolerate the imposed noise and outliers. However, the reconstructed images with weighting parameters larger than 0.3 offer higher robustness against noise and outliers.

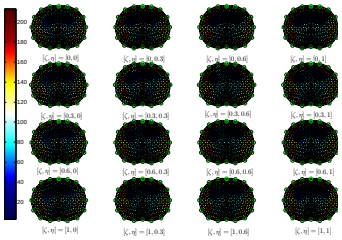

Figure 3: Clinical results of applying the proposed generalized PDIPM with weighted L1 and L2 norms over EIT lung data achieved from a patient with healthy lungs.

Moreover, we show the first clinical results of applying weighted L1 and L2 norms over EIT lung data achieved for a patient with healthy lungs and a patient with acute lung injury (ALI). Positive end-expiratory pressure (PEEP) was applied on 7 patients with healthy lungs and 18 patients with ALI [4]. EIT lung data was acquired during the PEEP trial. Figure 3 represents difference EIT with the proposed generalized PDIPM framework when applied to EIT lung data frame taken at the maximum airway pressure (35 $cmH2O$) of the PEEP trial for a patient with healthy lungs (patient numbered 7 in our data base). The reconstructed images in figure 3 correctly show that the dependent lung areas are filled by air for both the right and left lungs, which is expected at the highest pressure of PEEP trial. The L2 norm based solution, located at the upper panel on the left corner in figure 3, is in fact the traditional Gauss-Newton method, where $[\zeta, \eta] = [0, 0]$. The L2 norms highly smooth out the solution and therefore create blobby images. This also shows the high vulnerability of L2 norm based penalty terms to measurement errors as they overly penalize, by squaring the mismatch terms, both measurement errors and useful physiological information. In contrary, the L1 norm based penalty terms sum up the absolute values of mismatch terms

and therefore are less prone to measurement errors and create sharp images with clear edges. The larger the weighting parameters, the higher the contribution of the L1 norms in the inverse solution will be. In figure 3, the reconstructed images with larger weighting values in the columns 2-4 are sharper images due to the higher contribution of the L1 norms in the inverse solution. The higher weighting values for image mismatch terms offer sharper images (row 1 in figure 3); however, the images suffer from data outliers (artifacts at the thorax boundary), due to having L2 norms on the data mismatch terms ($\zeta = 0$). The higher weighting values for data mismatch terms (column 1 in figure 3) produce robustness against data outliers; however, the images are smoothed out, due to imposing L2 norms on the image mismatch terms ($\eta = 0$).

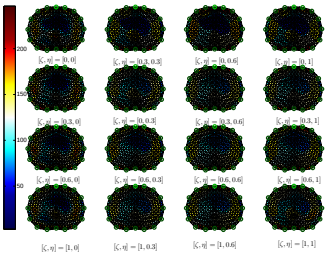

Figure 4: Clinical results of applying the proposed generalized PDIPM with weighted L1 and L2 norms over EIT lung data achieved from a patient with acute lung injury (ALI).

Figure 4 demonstrates the effect of different weighting parameters (ζ and η) on the reconstructed image from EIT lung data achieved on the inflation limb of PEEP trial where the airway pressure reaches to its highest value for a patient with ALI (patient numbered 18 in our data base). All reconstructed images clearly show the lungs malfunction due to a heterogeneous lung disease, which causes collapsed areas mostly in the lung dependent areas. Also, figure 4 indicates a decrease in the the lung volume, which is not normal at the plateau on the inflation limb of the PEEP trial.

5 Discussion

Functional EIT is a non-invasive, inexpensive imaging modality to image the regional ventilation distribution for long period of time. Difference EIT monitors lung impedance changes during ventilation and can be applied as a tool to help tune up the PEEP level. In this manuscript, we investigate the first clinical results of applying the generalized PDIPM with a combination of weighted L1 and L2 norms in producing quality EIT lung image. In clinical setting, there are several sources of errors in EIT data measurement, such as patient movement, sweating, and loose electrode connection, which create measurement errors. A reconstruction algorithm with sharp image and low vulnerability to the data outliers is desirable in clinical application of EIT. The proposed generalized PDIPM with weighted L1 and L2 norms can be applied in EIT clinical application to reconstruct sharp, quality images. It should be noted that one of the main difficulty of EIT image reconstruction is the high dependency of its inverse solution to the hyperparameter selection. In this study, we used L-curve method to tune the hyperparameter for every weighting combination applied in our implementation. However, there exist several other hyperparameter selection algorithms which could be investigated instead of L-curve method. Also, we have not used the available EIT motion compensation algorithms in our implementation. We expect the reported results in this manuscript to become less noisy if a motion compensation algorithm is applied.

6 Conclusion

We derive a generalized PDIPM framework which mixes the L1 norms and the L2 norms on both the data and the regularization terms of an inverse problem. To reach to the maximum generality, the norms are weighted to enclose the maximum number of possible categories of inverse problems. The classical inverse problems such as L2L2, L1L2, L2L1, and L1L1 problems are a sub-domain of the proposed generalized inverse problem where the weighting factors are selected accordingly. The generalized solution of the proposed inverse problem is derived using the PDIPM framework. EIT is selected as an instance of ill-posed non-linear inverse problem. We discuss the effectiveness of different combination of weighted norms (L1 and L2 norms) under two different measurement conditions on EIT simulated data (added noise and outliers). We also assess the performance of the proposed generalized PDIPM on clinical data achieved from EIT system. We discuss that the achieved clinical results of the proposed generalized PDIPM are plausible and also found that the assignment of larger values to the weighting parameters (ζ and η) is beneficial to produce sharp and less noisy images in clinical application of EIT for lung imaging.

References

[1] K. D. Andersen, E. Christiansen, A. Conn, and M. L. Overton. An efficient primal-dual interior-point method for minimizing a sum of Euclidean norms. *SIAM J. on Scientific Computing*, 22:243–262, 2000.

[2] J. Nocedal and S. J. Wright. *Numerical Optimization*. Springer, 1999.

[3] P. Rahmati, M. Soleimani, S. Pulletz, I. Frerichs, and A. Adler. Level-set-based reconstruction algorithm for eit lung images: first clinical results. *Journal on Physiological Measurement*, 33:739, 2012.

[4] M. Kott G. Elke B. Gawelczyk D. Schdler G. Zick N. Weiler I. Frerichs S. Pulletz S, A. Adler. Regional lung opening and closing pressures in patients with acute lung injury. *Journal of Critical Care*, 2011.

[5] A. Tarantola. *Inverse problem theory and methods for model parameter estimation*. Society for Industrial Mathematics, 2005.